AIP Journal of Applied Physics

Modelling the acoustical response of lossy lamella-crystals

J. Christensen, N. A. Mortensen, and M. Willatzen

Citation: Journal of Applied Physics **116**, 163508 (2014); doi: 10.1063/1.4898808
View online: http://dx.doi.org/10.1063/1.4898808
View Table of Contents: http://scitation.aip.org/content/aip/journal/jap/116/16?ver=pdfcov
Published by the AIP Publishing

JOURNAL OF APPLIED PHYSICS **116**, 163508 (2014)

Modelling the acoustical response of lossy lamella-crystals

J. Christensen,[a] N. A. Mortensen, and M. Willatzen
Department of Photonics Engineering, Technical University of Denmark, DK-2800 Kgs. Lyngby, Denmark

(Received 9 April 2014; accepted 9 October 2014; published online 24 October 2014)

The sound propagation properties of lossy lamella-crystals are analysed theoretically utilizing a rigorous wave expansion formalism and an effective medium approach. We investigate both supported and free-standing crystal slab structures and predict high absorption for a broad range of frequencies. A detailed derivation of the formalism is presented, and we show how the results obtained in the subwavelength and superwavelength regimes qualitatively can be reproduced by homogenizing the lamella-crystals. We come to the conclusion that treating this structure within the metamaterial limit only makes sense if the crystal filling fraction is sufficiently large to satisfy an effective medium approach. © *2014 AIP Publishing LLC*. [http://dx.doi.org/10.1063/1.4898808]

I. INTRODUCTION

The complex interactions of sound with periodic structures host a wealth of fascinating wave propagating phenomena. It is the ability to control the motion and direction of sound in most unusual and counter-intuitive ways that has sparked a great deal of interest within the condensed-matter and material research communities both from a theoretical and experimental point of view. The formation of acoustic band gaps, which are spectral frequency regions of forbidden sound propagation and in direct analogy to band gaps in electronic structures and photonic crystals, holds great promise in the design of reflective, mirror-like sound barriers. Reflection and absorption characteristics of finite periodic structures depend very much on the right choice of the host and inclusion material, the crystal symmetry but also the operating frequency range, and provide insight into several fascinating effects. Among them, we can name the discovery of the anomalous Doppler effect, acoustic analogue of the Zitterbewegung effect such as Dirac cones in phononic crystals and holey honeycomb structures.[1–4]

Metamaterials, on the other hand, are in no ways inferior to phononic crystals. Although many exotic properties arise from resonance behaviour, the landscape of properties one is capable to archive by the use of metamaterial is very broad. The vast range of phenomena associated with tailored acoustic properties have led to applications of acoustic focusing,[5–7] waveguiding,[8,9] cloaking,[10–12] negative refraction,[13] and resonant transmission through hole arrays,[14–17] all attracting a major focus of attention. Cloaks have been observed for both elastic and acoustic waves, including acoustic carpets.[18–20] Many of the named findings have been made possible by the utilization of locally resonating structures, but recently it has been found that perforated structures do the same job by providing flexible and eased tunability.[7,18,19,21–23]

In this work, we unify the concepts behind phononic crystals and metamaterials by designing a structured functional material acting as a highly absorptive layer. It is known that many intriguing metamaterial properties, such as resonance-based absorption, suffer in the performance when it comes to the need of pronounced bandwiths.[24] To counteract on this drawback, we propose an artificial crystal based on lossy lamellas that constitutes a broadband system, since the wave interaction originates from diffraction effects as we focus the study far beyond the long wavelength limit.[25] The goal within this work is twofold: first, we present a mathematical formalism that is capable to capture the entire scattering properties of lossy lamella crystals, both backed and free-standing; and second, we will discuss the possibility to homogenize these structures by means of effective material parameters.

II. RIGOROUS WAVE EXPANSION FORMALISM

The complex wave scattering is derived by a rigorous expansion formalism. This technique is based on the coupling of free space diffracted Bloch waves to waveguide resonances that at the same time are decomposed into periodic Bloch modes. In doing so, we examine both symmetric and asymmetric structures, that is, a free-standing periodic lossy slab and one which is backed by an impenetrable support, see Fig. 1. The schematics illustrate how waves irradiate onto the slab; hence, we must consider in the region of the crystal-slab both in-plane and out-of-plane wave propagation. In conventional phononic crystal studies, wave propagation is confined along the in-plane ($z = 0$) orientation and the wave pressure within the unit cell is fully represented by a Bloch solution. In the present case, however, we compose the solution from in-plane Bloch waves and out-of-plane harmonic pressure waves

$$p = e^{i\omega t} e^{iqz} \sum_G p^G e^{i(k_x+G)x}. \tag{1}$$

This construction comprise q, the out-of-plane wave vector, $k_x + G$ the in-plane wave vector with $G = G_x = n\frac{2\pi}{a}\hat{x}$, where n runs from $[-\infty;\infty]$, p^G is the eigenvector, and $k_x = k_0 \sin\theta$. The wave equation for inhomogeneous materials is solved by expanding the wave solution and the complex material parameters in the reciprocal lattice space. By doing this, we consider material losses via complex values of

[a]jochri@fotonik.dtu.dk

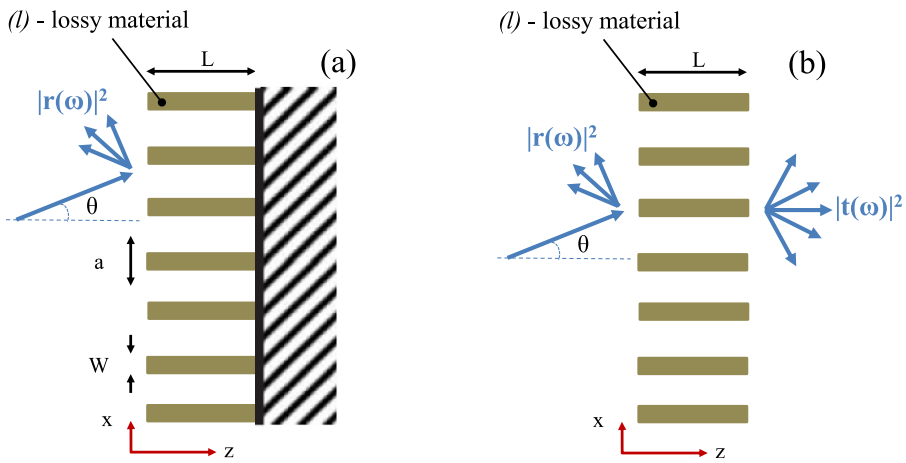

FIG. 1. Schematics of the two structures under investigation. A lossy material with a complex mass density ρ_l and bulk modulus K_l is cut into lamella and entirely surrounded by air (ρ, K). Free-space wave radiation is incident from left to right onto an (a) asymmetric and a (b) symmetric configuration. We denote the size of the unit cell a and the width of the lamella W.

the mass density ρ_l and bulk modulus K_l and end up with the following set of equations:

$$\sum_{G'}\left[\frac{1}{\rho_{G-G'}}\left(D_{G,G'}+q^2\right)-\omega^2\frac{1}{K_{G-G'}}\right]p^{G'}=0, \tag{2}$$

where $D_{G,G'}=(k_x+G)\cdot(k_x+G')$. Whether we consider a backed slab (Fig. 1(a)) or free slab (Fig. 1(b)), the cavity waveguide modes of order j are collected over the reciprocal lattice vectors, as shown below. In this respect, we can write the overall modal pressure within this region for the backed slab as

$$p=2\sum_G\sum_j p_j^G B_j\cos\left(q_j(z-L)\right)e^{i(k_x+G)x}, \tag{3}$$

where B_j represents the jth modal amplitude. Upon differentiating Eq. (3) with respect to z, it can be shown that the acoustic normal velocity vanishes at the rigid back-support, $z=L$. Next, we write the corresponding modal pressure for the free slab, as follows:

$$p=\sum_G\sum_j p_j^G\left(A_je^{iq_jz}+B_je^{-iq_jz}\right)e^{i(k_x+G)x}. \tag{4}$$

In order to present a physical picture with the expressions given by Eqs. (3) and (4), one has to appreciate that the pressure Bloch waves spread across the infinite lattice associates harmonic waves of order j in the perpendicular direction to the lattice. The shape of these waves depends very much on the boundary conditions linked to asymmetric (Fig. 1(a), Eq. (3)) or symmetric (Fig. 1(b), Eq. (4)) configurations. Before continuing along this line, we specify the region of radiation where the incident and reflected portion of the pressure wave, shared by both configurations, is written as

$$p=e^{ik_xx}e^{ik_zz}+\sum_G r_Ge^{i(k_x+G)x}e^{-ik_z^Gz}, \tag{5}$$

where $k_z^G=\sqrt{k_0^2-(k_x+G)^2}$ and $k_z=k_z^{G=0}=\sqrt{k_0^2-k_x^2}$ are the free-space wavenumbers perpendicular to the crystal interface comprising diffractive and specular radiation, respectively. Finally, in the symmetric case, additionally we consider transmission of the wave, hence, sound emerging the slab is written as

$$p=\sum_G t_Ge^{i(k_x+G)x}e^{ik_z^G(z-L)}. \tag{6}$$

We begin with the asymmetric case, the simpler one, since it contains a single interface only ($z=0$). At that interface, we impose continuity of the pressure p and the normal velocity $\frac{1}{\rho}\partial_zp$, thus, we write

$$\begin{aligned}\delta_{0G}+r_G&=2\sum_j p_j^GB_j\cos\left(q_jL\right),\\ -k_z\delta_{0G}+k_z^Gr_G&=2i\rho\sum_{G'}\sum_j\frac{q_jp_j^{G'}}{\rho_{G-G'}}B_j\sin\left(q_jL\right),\end{aligned} \tag{7}$$

where ρ is the mass density of the background fluid (air). In Eq. (7), we can eliminate the reflection coefficient r_G such that the only unknown to be solved for is B_j: The corresponding linear set of equations becomes

$$\sum_j\left(i\rho\sum_{G'}\frac{q_jp_j^{G'}}{\rho_{G-G'}}\sin\left(q_jL\right)-k_z^Gp_j^G\cos\left(q_jL\right)\right)B_j=-k_z\delta_{0G}. \tag{8}$$

Ultimately, we can write the expression for the reflection coefficient

$$r_G=2\sum_j p_j^GB_j\cos\left(q_jL\right)-\delta_{0G}, \tag{9}$$

from which we derive the overall absorption

$$A=1-\sum_G\mathrm{Re}\left(\frac{k_z}{k_z^G}\right)|r_G|^2=1-|r(\omega)|^2, \tag{10}$$

where $|r(\omega)|^2$ is the reflectance, the intensity of the back-reflected wave compared to the impinging flux. In a similar way, we can solve the complex scattering coefficients for the free standing slab. Naturally, we are going to deal with two interfaces. At $z=0$, we have

$$\sum_j \left(\rho \sum_{G'} \frac{q_j p_j^{G'}}{\rho_{G-G'}} (A_j - B_j) + k_z^G p_j^G (A_j + B_j) \right) = 2k_z \delta_{0G}, \tag{11}$$

and at the far-side of the slab ($z = L$)

$$\sum_j \left(\rho \sum_{G'} \frac{q_j p_j^{G'}}{\rho_{G-G'}} \left(A_j e^{iq_j z} - B_j e^{-iq_j z}\right) - k_z^G p_j^G \left(A_j e^{iq_j z} + B_j e^{-iq_j z}\right) \right) = 0, \tag{12}$$

which are obtained upon eliminating the scattering coefficients. These are the complex reflection

$$r_G = \sum_j p_j^G (A_j + B_j) - \delta_{0G}, \tag{13}$$

and transmission

$$t_G = \sum_j p_j^G (A_j e^{iq_j L} + B_j e^{-iq_j L}) \tag{14}$$

coefficients. With these equations, we can now write the expression for the overall absorption

$$A = 1 - \sum_G \mathrm{Re}\left(\frac{k_z}{k_z^G}\right) |r_G|^2 - \sum_G \mathrm{Re}\left(\frac{k_z}{k_z^G}\right) |t_G|^2. \tag{15}$$

The missing unknowns, which are weighting the scattering coefficients of Eqs. (13) and (14), can be found upon defining the modal fields $\psi_j = A_j - B_j$ and $-\psi_j' = A_j e^{iq_j z} - B_j e^{-iq_j z}$. By doing so, we further reduce Eqs. (11) and (12) into the following system:

$$\begin{bmatrix} \Omega - \epsilon & V \\ V & \Omega - \epsilon \end{bmatrix} \begin{bmatrix} \psi_j \\ \psi_j' \end{bmatrix} = \begin{bmatrix} I \\ 0 \end{bmatrix}, \tag{16}$$

with $\Omega = i\rho \sum_{G'} \frac{q_j p_j^{G'}}{\rho_{G-G'}}$, $\epsilon = \frac{k_z^G p_j^G}{\tan(q_j L)}$, $V = -\frac{k_z^G p_j^G}{\sin(q_j L)}$, and $I = 2ik_z \delta_{0G}$. Note that Eq. (8) could be recast in a similar compact set of equations, as presented by Eq. (16). With these expressions, we are able to compute wave interaction of 1D lossy lemalla-crystals, although extensions into 2D would be readily possible as well. At this stage, we wish to stress that this formalism differs substantially from the one used to model extraordinary transmission of sound. For subwavelength apertures in rigid metallic screens, plane waves are coupled to slit or hole eigenmodes only and the formalism does not take into consideration the penetration of acoustic energy into the metallic region at all.[17]

Next, we apply an effective medium theory (EMT) in order to examine the possibility to homogenize the lossy periodic structure. Principally, we are dealing with a Bragg stack from which well known expressions are applied to describe effective mass densities and bulk moduli in the long-wavelength regime.[26] This structure constitutes a uniaxial anisotropic material with effective parameters, as we will find below. If we define the crystal filling fraction to be $\mathrm{f} = \mathrm{W}/a$, we can write these effective parameters as

$$\rho_{\mathrm{eff}}^x = \mathrm{f}\rho_l + (1 - \mathrm{f})\rho,$$
$$\frac{1}{\rho_{\mathrm{eff}}^z} = \frac{\mathrm{f}}{\rho_l} + \frac{1 - \mathrm{f}}{\rho},$$
$$\frac{1}{K_{\mathrm{eff}}} = \frac{\mathrm{f}}{K_l} + \frac{1 - \mathrm{f}}{K}. \tag{17}$$

It is also straightforward, upon assuming plane monofrequency wave propagation and homogeneous media, to write the generalized dispersion relation

$$k_z' = \sqrt{\rho_{\mathrm{eff}}^z} \sqrt{\frac{\omega^2}{K_{\mathrm{eff}}} - \frac{k_x^2}{\rho_{\mathrm{eff}}^x}}. \tag{18}$$

With these expressions, we can define the Fresnel's coefficients at the interfaces of an effective anisotropic fluid slab. The first reflection and transmission coefficients the wave encounters at the air-slab interface read

$$r_{21} = \frac{\rho_{\mathrm{eff}}^z k_z - \rho k_z'}{\rho_{\mathrm{eff}}^z k_z + \rho k_z'}, \quad t_{12} = \frac{2\rho_{\mathrm{eff}}^z k_z}{\rho_{\mathrm{eff}}^z k_z + \rho k_z'}, \tag{19}$$

and similarly we can write the other ones at the remaining interfaces, which we gather by the overall reflection coefficient after multiple round-trips

$$r(\omega) = r_{21} + \frac{\tau_{12} r_{32} \tau_{21} e^{2ik_z' L}}{1 - r_{32} r_{12} e^{2ik_z' L}}. \tag{20}$$

Equation (20) is a universal expression for the reflection coefficient and can be applied for both structures depicted in Fig. 1. For the asymmetric system however, we set $r_{32} = 1$. Both for the exact numerical simulation and the present EMT we need to specify the complex dispersive material parameters to account for losses. In the following, we will exemplify this for the symmetric and asymmetric structure.

III. RESULTS AND DISCUSSION

In Fig. 2, we begin by simulating the spectral dependence of the absorption expressed by Eq. (10) at normal incidence ($k_x = 0$) for a backed porous lamella-crystal slab. As indicated, we investigate three different filling fractions that have been realized by keeping W fixed but varying the size of the unit cell a. Akin to our recent experiments, we vary the separation of adjacent lamellas to modify the filling fraction rather than keeping the lattice constant fixed.[25] We consider dispersive porous foam lamellas and for the calculations we apply well known effective expressions for the complex parameters ρ_l and K_l therein.[27] The overall predicted absorption is very high and larger than 0.9 for a broad range of frequencies for the cases where $\mathrm{f} = 40\%$ and 70%. Sharp diffraction features associated with momentum transfer of sound to the lattice (lattice singularities, $|k_x + G| = \omega/c$) give rise to high reflections (low absorptions) and in the case where $\mathrm{f} = 20\%$, the overall performance is less pronounced in terms of high absorption. These lattice features naturally shift towards lower frequencies when the filling fraction is lowered. From Eq. (20), we also calculate the homogenized absorption

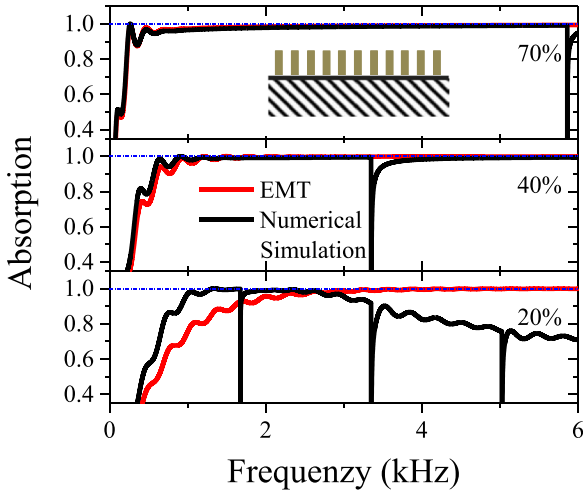

FIG. 2. Absorption spectrum for normal incidence sound radiation for a backed crystal slab with $L = 0.5$ m and W $= 0.04$ m. We compute the acoustic response for three different crystals with filling fraction, f $= 20\%$, 40%, and 70% as indicated and compare results obtained based on an EMT and exact numerical simulations.

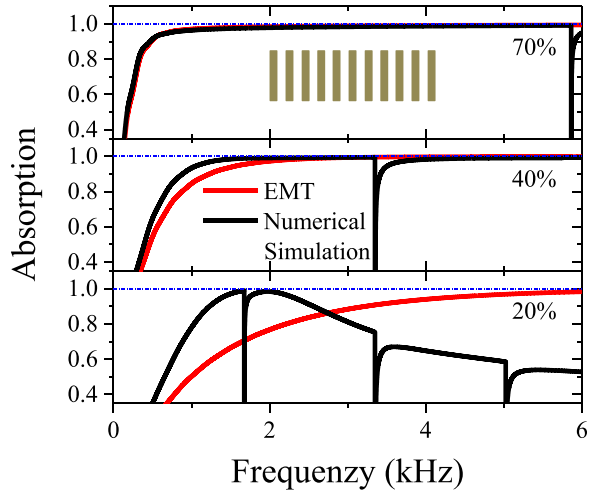

FIG. 3. Absorption spectrum for normal incidence sound radiation for a free standing crystal slab with $L = 0.5$ m and W $= 0.04$ m. We compute the acoustic response for three different crystals with filling fraction, f $=$ 20%, 40%, and 70% as indicated and compare results obtained based on an EMT and exact numerical simulations.

$A = 1 - |r(\omega)|^2$ based on the EMT. It is evident that the lattice singularities that are induced by coherent diffraction through the entire crystal cannot be captured by the EMT. Despite the good agreement between the exact numerical simulations and the EMT-based approximation even when $\lambda < a$, the effective medium approach becomes less accurate as scattering effects become more significant, which is the case for a smaller filling fraction. For example, when the unit cell at f $= 70\%$ is predominantly occupied by the porous material, less scattering in the air region inside the crystal takes place and good agreement with the EMT is reached. Contrary to this however, when f $= 20\%$, we have large spacings between adjacent lamellas and in fact little lossy material within the unit cell. The consequential increase of scattered sound leaves the EMT invalid for that case and low filling fractions, in general. Hence, although dominating diffraction features appear in the spectrum that cannot be captured by an EMT, overall there seems to be good qualitative agreement for porous-lamella crystals treated as a homogenized structure when the filling fraction is large.

In the same framework, we investigate the absorption by means of exact numerics and EMT for a free standing crystal slab as rendered in Fig. 3. We have conducted simulations for the exact same geometries as in the former case. In Fig. 3, we plot Eq. (15) and solve for A in Eq. (20), now with $r_{32} \neq 1$, after taking into consideration the transmission $t(\omega)$ as well. First, upon inspecting the full numerical simulations for both the asymmetric, Fig. 2, and the symmetric case, Fig. 3, we see that the removal of the rigid back supports also removes oscillating features in the overall absorption spectra. It seems however that the absorption spectra are slightly higher when a back support is present. Although we are using the exact same material and geometries, this finding is expected as we equivalently deal with a structure of twice the path length in the asymmetric case as opposed to the symmetric configuration. In other words, the sound intensity attenuates stronger upon leaving the slab as it has travelled a longer path. As in the previous case, there is qualitatively good agreement between the EMT and numerical simulations for higher filling fractions only. At f $= 20\%$ again, EMT becomes inaccurate. As we mentioned before, to ease an experimental verification with different filling fractions we held the lamella width W unchanged and varied the lattice constant a. Conventionally, one would do the opposite

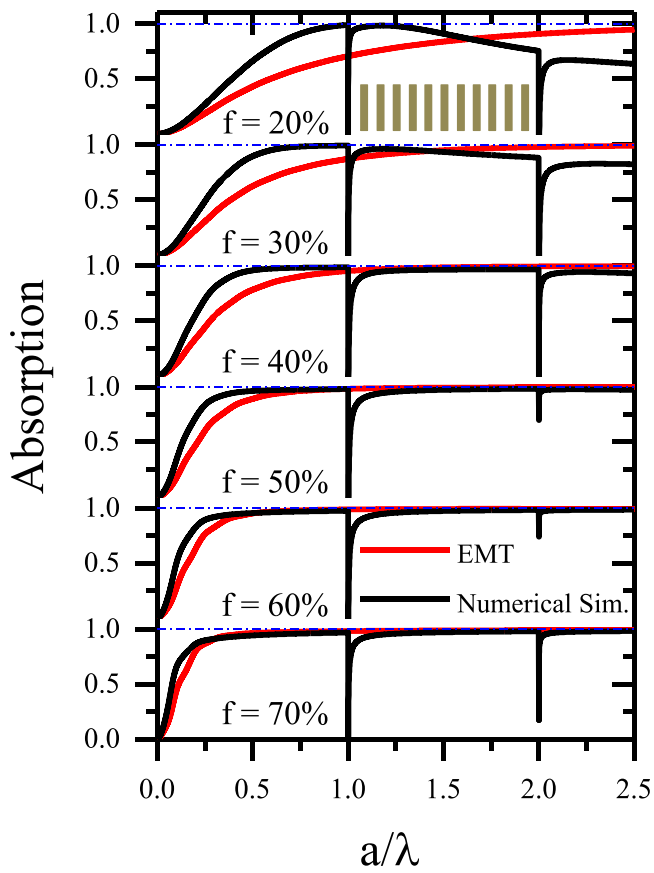

FIG. 4. Absorption spectrum for normal incidence sound radiation for a free standing crystal slab with $L = 0.5$ m and $a = 0.2$ m. As opposed to the previous examples, we keep the lattice constant fix but vary the lamella width W. Exact numerical simulations are compared to the EMT.

and plotting against the normalized frequency, that is, the absorption as a function of the lattice constant-to-wavelength ratio. In this way, the absorption spectra for different crystal densities can be compared directly on the same scale. We take the example of the free-standing crystal-slab and lock the lattice constant as captured in Fig. 4. As expected do the lattice constants remain spectrally unaffected, and as we reported earlier,[25] when lowering the filling fraction the maximal absorption peak (not the width) increases as can seen under close inspection of the numerical results in Fig. 4. Reminiscent to the previous discussion, even when focusing in the deep metamaterial regime ($\lambda > a$), the EMT becomes meaningful only when the filling fraction is relatively high. Although the lattice constant is kept small compared to the free-space wavelength, the interfacial distance between neighbouring lamellas determine the number of Bloch waves needed to be included in the expansion. In other words, convergence is obtained faster when the filling fraction is high.

IV. CONCLUSION

In summary, we have presented a compact formalism capable to describe the complex wave interaction in finite lossy lamella-crystals, both in a symmetric and asymmetric configuration. We have theoretically shown that high absorption is possible within these systems but that the filling fraction of the crystal plays a crucial role. Since the derivation of a rigorous model motivated the present study, we also investigated the possibility to treat the structure within the long wavelength regime via an EMT. We found that despite some diffraction features in the absorption spectrum, lossy lamella crystals with high filling fractions can be homogenized as supported by good agreement between exact numerical simulations obtained by our theory and an EMT.

ACKNOWLEDGMENTS

J.C. gratefully acknowledges financial support from the Danish Council for Independent Research and a Sapere Aude Grant (12-134776).

[1] X. Hu, Z. Hang, J. Li, J. Zi, and C. T. Chan, Phys. Rev. E **73**, 015602(R) (2006).
[2] X. Zhang and Z. Liu, Phys. Rev. Lett. **101**, 264303 (2008).
[3] F. Liu, Y. Lai, X. Huang, and C. T. Chan, Phys. Rev. B **84**, 224113 (2011).
[4] D. Torrent and J. Sanchez-Dehesa, Phys. Rev. Lett. **108**, 174301 (2012).
[5] S. Guenneau, A. Movchan, G. Petursson, and S. A. Ramakrishna, New. J. Phys. **9**, 399 (2007).
[6] Z. He, F. Cai, Y. Ding, and Z. Liu, Appl. Phys. Lett. **93**, 233503 (2008).
[7] J. Christensen and F. J. G. de Abajo, Phys. Rev. Lett. **108**, 124301 (2012).
[8] J. Christensen, P. A. Huidobro, L. Martin-Moreno, and F. J. Garcia-Vidal, Appl. Phys. Lett. **93**, 083502 (2008).
[9] J. Zhu, Y. Chen, X. Zhu, F. J. Garcia-Vidal, X. Yin, W. Zhang, and X. Zhang, Sci. Rep. **3**, 1728 (2013).
[10] G. W. Milton, M. Briane, and J. R. Willis, New. J. Phys. **8**, 248 (2006).
[11] H. Chena and C. T. Chan, Appl. Phys. Lett. **91**, 183518 (2007).
[12] A. D. S. G. G. Dupont, M. Farhat, and S. Enoch, Wave Motion **48**, 483 (2011).
[13] L. Fok and X. Zhang, Phys. Rev. B **83**, 214304 (2011).
[14] B. Hou, J. Mei, M. Ke, Z. Liu, J. Shi, and W. Wen, J. Appl. Phys. **104**, 014909 (2008).
[15] H. Estrada, F. J. G. de Abajo, P. Candelas, A. Uris, F. Belmar, and F. Meseguer, Phys. Rev. Lett. **102**, 144301 (2009).
[16] F. J. G. de Abajo, H. Estrada, and F. Meseguer, New. J. Phys. **11**, 093013 (2009).
[17] J. Christensen, L. Martin-Moreno, and F. J. Garcia-Vidal, Phys. Rev. Lett. **101**, 014301 (2008).
[18] B.-I. Popa, L. Zigoneanu, and S. A. Cummer, Phys. Rev. Lett. **106**, 253901 (2011).
[19] N. Stenger, M. Wilhelm, and M. Wegener, Phys. Rev. Lett. **108**, 014301 (2012).
[20] L. Sanchis, V. M. García-Chocano, R. Llopis-Pontiveros, A. Climente, J. Martínez-Pastor, F. Cervera, and J. Sánchez-Dehesa, Phys. Rev. Lett. **110**, 124301 (2013).
[21] M. Farhat *et al.*, Appl. Phys. Lett. **96**, 081909 (2010).
[22] Y. Xie, B. Popa, L. Zigoneanu, and S. A. Cummer, Phys. Rev. Lett. **110**, 175501 (2013).
[23] Z. Liang, T. Feng, S. Lok, F. Liu, K. B. Ng, C. H. Chan, J. Wang, S. Han, S. Lee, and J. Li, Sci. Rep. **3**, 1614 (2013).
[24] J. Mei, G. Ma, M. Yang, Z. Yang, W. Wen, and P. Sheng, Nat. Commun. **3**, 756 (2012).
[25] J. Christensen, V. Romero-Garcia, R. Pico, A. Cebrecos, F. J. de Abajo, N. A. Mortensen, M. Willatzen, and V. J. Sanchez-Morcillo, Sci. Rep. **4**, 4674 (2014).
[26] D. Torrent and J. Sanchez-Dehesa, New. J. Phys. **10**, 023004 (2008).
[27] D. Lafarge, P. Lemarinier, J. F. Allard, and V. Tarnow, J. Acoust. Soc. Am. **102**, 1995 (1997), with the macroscopic parameters: $\phi = 0.94$, $\alpha_\infty = 1$, $\sigma = 20\,000\ \mathrm{Nm}^{-4}\,\mathrm{s}$, and $\Lambda = \Lambda' = 0.41\ \mu\mathrm{m}$.